The Journal of Infectious Diseases

MAJOR ARTICLE

Plasmodium falciparum-CD36 Structure-Function Relationships Defined by Ortholog Scanning Mutagenesis

Ana Cabrera,[1] Dante Neculai,[2] Vanessa Tran,[1] Thomas Lavstsen,[3] Louise Turner,[3] and Kevin C. Kain[1,4]

[1]SAR Laboratories, Sandra Rotman Centre, Toronto General Hospital-University Health Network, Ontario, Canada; [2]Department of Cell Biology, Zhejiang University, School of Basic Medical Sciences, Hangzhou, People's Republic of China; [3]Centre for Medical Parasitology, Department of International Health, Immunology and Microbiology, University of Copenhagen and Department of Infectious Diseases, Rigshospitalet, Denmark; [4]Tropical Disease Unit, Division of Infectious Diseases, Department of Medicine, University of Toronto, Ontario, Canada

Background. The interaction of *Plasmodium falciparum*-infected erythrocytes (IEs) with the host receptor CD36 is among the most studied host-parasite interfaces. CD36 is a scavenger receptor that binds numerous ligands including the cysteine-rich interdomain region (CIDR)α domains of the erythrocyte membrane protein 1 family (PfEMP1) expressed on the surface of IEs. CD36 is conserved across species, but orthologs display differential binding of IEs.

Methods. In this study, we exploited these differences, combined with the recent crystal structure and 3-dimensional modeling of CD36, to investigate malaria-CD36 structure-function relationships and further define IE-CD36 binding interactions.

Results. We show that a charged surface in the membrane-distal region of CD36 is necessary for IE binding. Moreover, IE interaction with this binding surface is influenced by additional CD36 domains, both proximal to and at a distance from this site.

Conclusions. Our data indicate that subtle sequence and spatial differences in these domains modify receptor conformation and regulate the ability of CD36 to selectively interact with its diverse ligands.

Keywords. host-parasite interaction; infected erythrocytes; ortholog swap mutagenesis; scavenger receptor.

Plasmodium falciparum malaria remains a leading cause of childhood mortality responsible for an estimated 445 000 deaths in 2016 [1–3]. *Plasmodium falciparum* virulence depends on the expression of a diverse *var* gene family encoding the erythrocyte membrane protein 1 family (PfEMP1), which is exposed on the infected erythrocyte (IE) surface. The *var* gene family undergoes transcriptional switching to modify the antigenic properties and adhesive phenotype of the IE and confers its ability to sequester in the microvasculature [4–6].

PfEMP1 are large proteins that contain 2 to 10 adhesive domains termed Duffy binding-like and cysteine-rich interdomain region (CIDR) domains [4–6]. Of the various host receptors that engage PfEMP1 proteins, the interaction with the scavenger receptor CD36 is among the most studied. CIDRα2–6 domains have been reported to mediate the interaction between PfEMP1 and CD36 [7–9].

CD36 is a class B scavenger receptor that belongs to a larger superfamily of pattern recognition receptors (PRRs). CD36 binds a diverse range of ligands including both pathogen-associated molecular patterns (PAMPs) and modified self-molecules [10]. CD36 can recognize PAMPs present directly on pathogens or expressed on their infected host cells including specific lipids in bacterial cell walls and parasite proteins embedded in the IE surface [10, 11]. These CD36-pathogen interactions mediate opsonin-independent uptake by monocytic cells [12]. CD36 also recognizes and internalizes endogenously derived ligands including modified lipoproteins such as oxidized low-density lipoprotein (oxLDL) [11]. CD36 has been shown to form complexes with multiple coreceptors and membrane proteins including Toll-like receptors ([TLR]2, TLR4, TLR6) [11, 13].

The role of CD36 in both homeostasis and disease has been studied for over 40 years, but the relationship between CD36 and malaria has been controversial [14]. Recent evidence indicates that CD36 binding is generally associated with milder infection, whereas binding to the endothelial protein C receptor (EPCR) is linked to severe disease [15].

The lack of structural data on this class of receptors has limited an understanding of how CD36 selectively engages and differentially responds to its diverse repertoire of ligands. Insights into these processes have been advanced by solving the crystal structure of the first member of this class of scavenger receptors (lysosomal integral membrane protein [LIMP]-2) and inferring the structure of CD36 by homology modeling [16]. CD36 forms a "hairpin-like" structure with a large ectodomain and 2 transmembrane domains. The ectodomain of CD36 is capped by a 3-α-helix bundle and apex region that contains an accumulation of cationic residues, proposed to function as a binding site for its polyanionic ligands, such as modified lipoproteins [16].

Received 28 July 2018; editorial decision 9 October 2018; accepted 12 October 2018; published online October 18, 2018.

Presented in part: American Society for Tropical Medicine and Hygiene, 2013, Washington, DC; BioMalPar, 2014, Heidelberg, Germany.

Correspondence: K. C. Kain, MD, FRCPC, Sandra Rotman Centre, Suite 10-351, Toronto Medical Discovery Tower, MaRS Centre, 101 College Street, Toronto M5G1L7, Canada (kevin.kain@uhn.ca).

The Journal of Infectious Diseases® 2019;219:945–54

DOI: 10.1093/infdis/jiy607

Cocrystallization studies of CIDRα2–6 domains and the CD36 ectodomain identified a conserved hydrophobic pocket on CIDRα peptides that bind a phenylalanine residue (F153) on CD36 [9]. However, these studies did not examine intact IE-CD36 interactions. Moreover, orthologs such as bovine CD36 (*b*CD36) express conserved cationic residues and F153 in the proposed binding surface, yet bind IEs poorly compared with human CD36 (*h*CD36). We hypothesized that the differential IE binding displayed by mammalian orthologs could be used to further refine CD36-malaria structure-function relationships [11]. In this study, we use an ortholog-substitution approach combined with recent structural data and CIDR peptides, to define regions important for IE binding.

METHODS

Sequences and Alignments

CD36 ortholog sequences were acquired from the National Center for Biotechnology Information (www.ncbi.nlm.nih.gov) and aligned using ClustalW (www.ebi.ac.uk/Tools/msa/clustalw2/): AAA16068.1 (*Homo sapiens*), AAH10262.1 (*Mus musculus*), AAH72543.1 (*Rattus norvegicus*), and AAI03113.1 (*Bos taurus*).

Cloning and Sequencing

Full-length *h*CD36 and mutants were cloned and sequenced as previously described [16]. *h*CD36 was used as template for cloning most human constructs with bovine-sequence insertions (See Supplementary Table 1 for templates and primer sequences) with a polymerase chain reaction (PCR) strategy using overlapping primers encompassing the desired mutation and the kanamycin cassette and amplified with CloneAmp HiFi PCR Premix (Clontech). The PCR products were purified, DpnI (NEB) digested, and ligated using In-Fusion HD cloning kit (Clonetech). *b*CD36 was amplified from the clone Image ID 7985341 (BioScience) and cloned into pEGFP-N1 vector. This construct was used as template for cloning bovine constructs with human-sequence insertions (see Supplementary Table 1). All constructs were sequence verified. All tested mutations, their backbone and associated figures are listed in Table 1.

Parasite Culture

Plasmodium falciparum MR4 strains E8B and CS2 strains were cultured in T-25 flasks with 5% hematocrit in complete Dulbecco's modified Eagle's medium (DMEM) with a microaerophilic environment (1% O_2, 5% CO_2, and rest N_2) as previously described [17].

Cell Culture and Transfection

CHO and Cos-7 cells were cultured to confluence in DMEM (Gibco) media with penicillin/streptomycin (Sigma) and 10% fetal bovine serum (Sigma) at 37°C and 5% CO_2. One million cells were plated in T25 flasks or 12-well plates with coverslips and transfected the next day using Polyethylenimine (PEI) (Polysciences, Inc.) as previously described [18]. Here, PEI was used in a 3:1 ratio with the plasmid deoxyribonucleic acid of interest. After 15-minute incubation, the mixture was added dropwise to the cells and incubated for 4 hours. Media was exchanged and the flasks were incubated for 24 hours. Experiments were standardized using both CHO and Cos-7 cell lines. CHO was used for flow cytometry experiments, and Cos-7 was used for cytoadherence assays and confocal microscopy.

Table 1. CD36 Mutations Included in this Manuscript

Backbone	Introduced Mutations	Associated Figures
hCD36 wild type	L158E, K164E, K166E, K164/166E	Figure 2
hCD36 wild type	Bovine Domains I and II	Figure 3
	Bovine Domain I: PQLPTMG, PQLP, P146	Figures 4–6
	Bovine Domain II: HGELAESSS, ESSS, S359	Figures 4–6
bCD36 wild type	Human Domains I and II	Figure 3
	Human Domain I: SHIQQVM, SHIQ, S146	Figures 4–6
	Human Domain II: YADVSDGNR, DGNR, G359	Figures 4–6

Surface Expression Determination

Surface expression of all the constructs was measured by flow cytometry using different anti-CD36 antibodies (Supplementary Figure 2): FA6-152 mouse immunoglobulin (Ig)G1 monoclonal antibody (mAb) (Beckman Coulter) and the phycoerythrin (PE)-conjugated IgM mAb (BD Biosciences). A CD36-binding peptide (CIDRa6_D3_IT4var12) specifically bound to all CD36 constructs and was also used to normalize expression of constructs.

Cytoadhesion Assay

Binding assays using non-IEs, CS2 (CSA binder) IEs, and E8B (CD36 binder) IEs were conducted. No binding was observed with any construct using noninfected and CS2 IEs (data not shown). E8B is a clone of ItG2 selected for adhesion to CD36, and *A4tres var* is reported as a dominant *var* transcript [19]. Any reference to IE is related to assays performed with E8B parasites. Mutant constructs are listed in Supplementary Table 1. Results are shown only for those mutations that showed significant differences compared with wild type (WT). Cytoadhesion assays were performed as described previously [20]. In brief, 24 hours after transfection, late-stage IEs were washed 3 times with Bis Tris saline (BTS) buffer (pH 6.8) and quantified. Culture was adjusted to 10% parasitemia in BTS, and 300 µL were added per well and continuously agitated for 90 minutes. Nonadherent cells were removed by aspiration, and coverslips were rinsed by submersion in phosphate-buffered saline (PBS). Cells were then fixed with 4% formaldehyde in PBS for 10 minutes and washed 3 times with PBS alone. Phycoerythrin-conjugated glycophorin A (BioLegend) was used to stain the IEs by 30-minute incubation. Coverslips were rinsed, and 4',6-diamidino-2-phenylindole was added for 5 minutes. Coverslips were mounted with fluoromount (Dako). Tiles were acquired for quantification using a ×25 0.8 numerical aperture (NA) oil-immersion lens using a

Zeiss AxioObserver Apotome equipped with an AxioCam camera, and images were obtained using the Zeiss ZEN software. Cells were visualized with a Zeiss ×63 1.4 NA oil-immersion lens using a Quorum spinning-disk confocal equipped with a back-thinned Hamamatsu EM-CCD camera (C9100-13); images were acquired by and processed with Perkin-Elmer Volocity software.

Cysteine-Rich Interdomain Region Peptide Binding

His-tagged CIDR peptides CIDRa1.1_D3_IT4var19, CIDRa5_D3_IT4var14, and CIDRa2.10_D2_IT4var30 were used as previously described [9]. Cells (0.5–1 million) were incubated with 100 μg/mL peptide in 2% bovine serum albumin for 60 minutes on ice. Cells were washed with PBS and incubated with 20 μg/mL anti-His mouse mAb (Abgent) for 30 minutes. Cells where then washed and incubated with 20 μg/mL anti-mouse Alexa Fluor 594 (Molecular Probes). After a final wash, cells were fixed with 1.6% formaldehyde in PBS for 10 minutes. Stained cells were washed and analyzed by flow cytometry.

Oxidized Low-Density Lipoprotein Binding

Cells (0.5–1 million) were stained with DiI-oxLDL (Intracel) for 30 minutes on ice. Cells where washed and fixed with 1.6% formaldehyde in PBS for 10 minutes. Stained cells were washed and transferred into polystyrene tubes for analysis by flow cytometry.

Flow Cytometry

Twenty-four hours after transfection, cells were detached from the flasks using 10 mM ethylenediaminetetraacetic acid (EDTA) for 10 minutes. Cells were stained for surface expression, CIDRα, or oxLDL binding, and 50 000 events were analyzed with a Becton Dickinson LSRII-CFI BGRV flow cytometer and Diva software. AbC Anti-Mouse Bead Kit (Invitrogen) was used for Alexa Fluor 594 compensation, and DiI (Molecular Probes) was used for DiI-oxLDL compensation.

Result Interpretation and Statistical Analysis

Flow cytometry data were analyzed using FlowJo X. Data were analyzed and graphed using GraphPad Prism 5 software. Graphs are presented with mean and standard deviation from a minimum of 3 independent experiments. All results were normalized to CD36 surface expression as indicated on the figure legend.

RESULTS

CD36-Infected Erythrocyte Interactions: The Role of Residues Previously Implicated in Ligand Binding

The putative tertiary structure and spatial relation between domains of CD36 have been modeled (Figure 1) [16]. A previously defined membrane-distal immunodominant region (155 to 183) lies in the helical bundle and apex region of the ectodomain [21]. To investigate a role for this region in binding IEs, we conducted a mutagenesis study of residues previously implicated

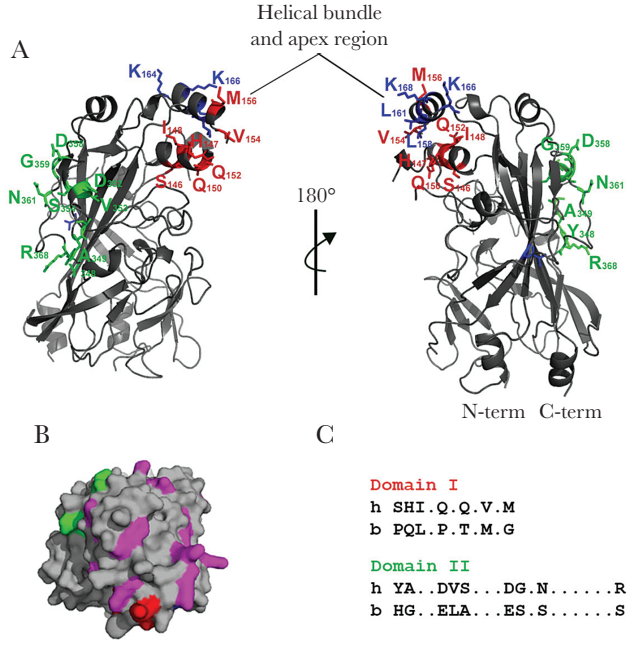

Figure 1. Human CD36 model. (A) Three-dimensional model based on the crystal structure of lysosomal integral membrane protein (LIMP)-2 [16]. Structure depicted in gray and domains of interest color coded. Domain I in red: SHIQQVM; domain II in green: YADVSDGNR; and other amino acids of interest in blue: T, LLKK. Model generated using PyMol. Helical bundle and apex region marked. (B) The cationic patch on the surface of CD36 viewed from the top. Cationic residues in the area depicted in magenta, whereas flanking domain I (red) and domain II (green) are highlighted. The rest of the structure is shown in gray. (C) Domain I and II alignment between human and bovine CD36 sequences.

in binding oxLDL [16]. We compared IE binding to WT and mutant CD36 molecules after correcting for any differences in receptor surface expression (Figure 2; Supplementary Figure 1). Mutation of the leucine residues at positions 158 (L158) and/or 161 (L161) to glutamic acid has previously been reported to abrogate oxLDL binding [16], whereas in our studies only L158E disrupted IE binding. Likewise, mutation of the cationic lysine residues at positions 164 and 166 (K164E and K166E) of CD36 eliminated IE binding, whereas single mutations did not (Figure 2, Supplementary Figure 1). Of note, point mutation of K164 also abrogated CD36 binding by the mAb FA6-152, which blocks IE binding by CD36 (Supplementary Figure 1).

CD36 Conservation: Mapping the Infected Erythrocyte Interaction Site by Ortholog Substitution

We examined the binding of *P falciparum* IEs by different CD36 orthologs. *h*CD36, mouse, and rat CD36 all supported IE binding, whereas *b*CD36 displays markedly reduced binding [20, 22] (Figure 3). These orthologs share more than 80% sequence identity. This sequence conservation, combined with differential IE binding, was used to investigate IE-CD36 binding interactions. Using multispecies sequence alignment, 2 areas of key divergence between bovine and the IE-binding orthologs were identified: domain I (residues 146–156, SHIQQVM) and domain II

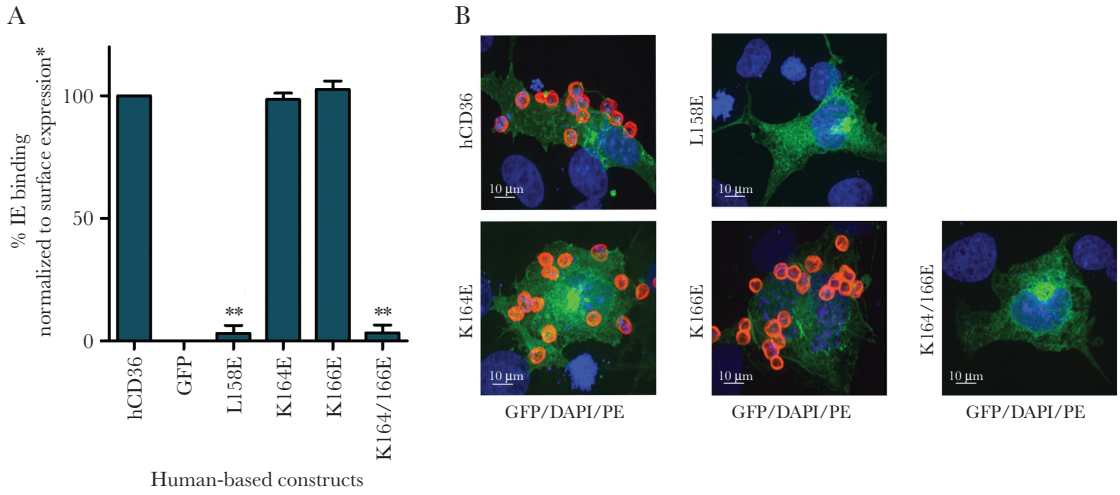

Figure 2. Infected erythrocyte (IE) binding by human CD36 mutants. (A) Quantification of IE binding assays on mutant CD36-green fluorescent protein (GFP). Infected erythrocyte binding of a selected experiment in triplicate is shown (mean + standard deviation), and statistical significance compared with *h*CD36 wild type (**, $P < .01$) is marked. Binding experiments were fixed and mounted for analysis using Zeiss Apotome. Tiles (10 × 10) were recorded using ×25 objective. (B) Confocal images (×63) of representative IE binding experiments of GFP fusion expressing cell lines (green). For fluorescent visualization, IEs were stained with phycoerythrin (PE)-conjugated antiglycophorin A as surface marker (red) and 4′,6-diamidino-2-phenylindole (DAPI) to stain the nucleus (blue). A 10-µm size bar is shown. Surface expression was normalized to BD555455 monoclonal antibody binding.

(residues 348–368, YADVSDGNR) (Figure 1 and Supplementary Figure 2). Secondary structure prediction tools [23] predict helixes in the *h*CD36 sequence within those regions of interest but not in *b*CD36, suggesting differential secondary structure. Domains I and II are predicted to be opposite each other on the *h*CD36 model with domain I buried within the helical bundle and domain II in an exposed region of the ectodomain (Figure 1).

Two Domains Regulate Differential Binding of Infected Erythrocytes by hCD36 Versus bCD36

An ortholog swap mutagenesis approach was used to examine the functional relevance of domains I and II. Amino acids of interest were exchanged between *h*CD36 and *b*CD36 to determine whether substituting residues between these orthologs would disrupt IE binding by *h*CD36 and, conversely, confer it

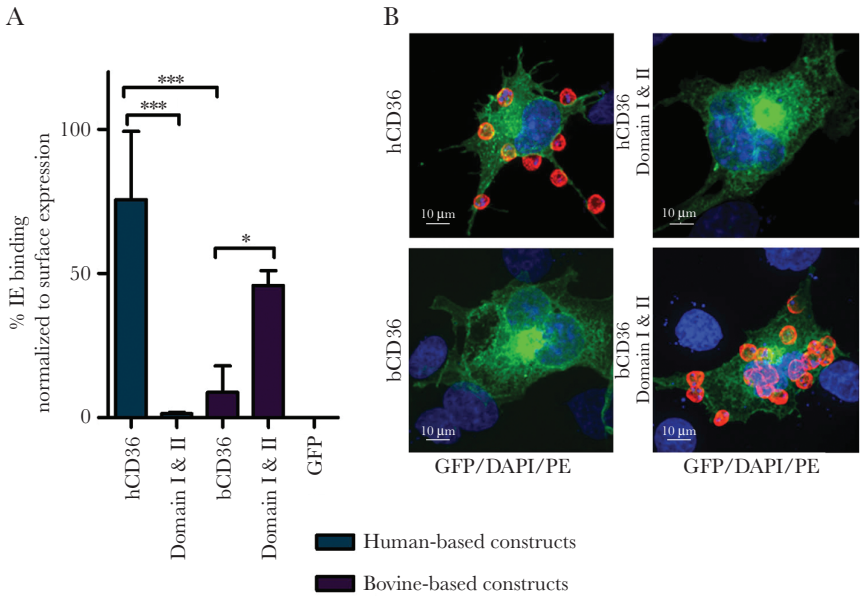

Figure 3. Infected erythrocyte binding by human and bovine CD36. (A) Quantification of IE binding of a representative experiment in triplicate (mean + standard deviation). Statistical significance compared with *h*CD36 (blue) and *b*CD36 (purple) wild type are shown (*, $P < .05$; ***, $P < .0001$). (B) Confocal images (×63) of representative parasite binding experiments of green fluorescent protein (GFP) fusion expressing cell lines (blue, 4′,6-diamidino-2-phenylindole [DAPI]; green, GFP fusion construct; red, antiglycophorin A-phycoerythrin [PE]). A 10-µm size bar is shown. *h*CD36 surface expression was normalized to FA6-152 monoclonal antibody binding, and *b*CD36 surface expression was normalized to CIDRα6_D3_IT4var12 binding (Supplementary Figure 2).

to *b*CD36, while preserving the overall tertiary structure and surface expression (Figure 1, Supplementary Figures 1 and 2). Two anti-CD36 mAbs and a specific CD36-binding CIDRα peptide were used to confirm surface expression (Supplementary Figure 1). The exchange of *h*CD36 domains I and II with the comparable regions from *b*CD36 resulted in the complete loss of IE binding (Figure 3). In contrast, replacing the bovine domains with the *h*CD36 domains I and II conferred IE binding to the *b*CD36 backbone (Figure 3). Independent examination of each domain showed that either *b*CD36 domain I or II disrupted IE binding, when used to replace the corresponding region in *h*CD36. Whereas substituting either domain I or II of *b*CD36, with the analogous region from *h*CD36, resulted in a significant increase in IE binding to *b*CD36 (Figure 4). Domain I exchange between the orthologs also disrupted binding of the *h*CD36 mAb BD555455 to *h*CD36 and conferred antibody binding to *b*CD36 (Supplementary Figure 2). These data indicate that exchanging these small domains between orthologs is sufficient to abrogate IE binding by *h*CD36 and to confer binding to *b*CD36.

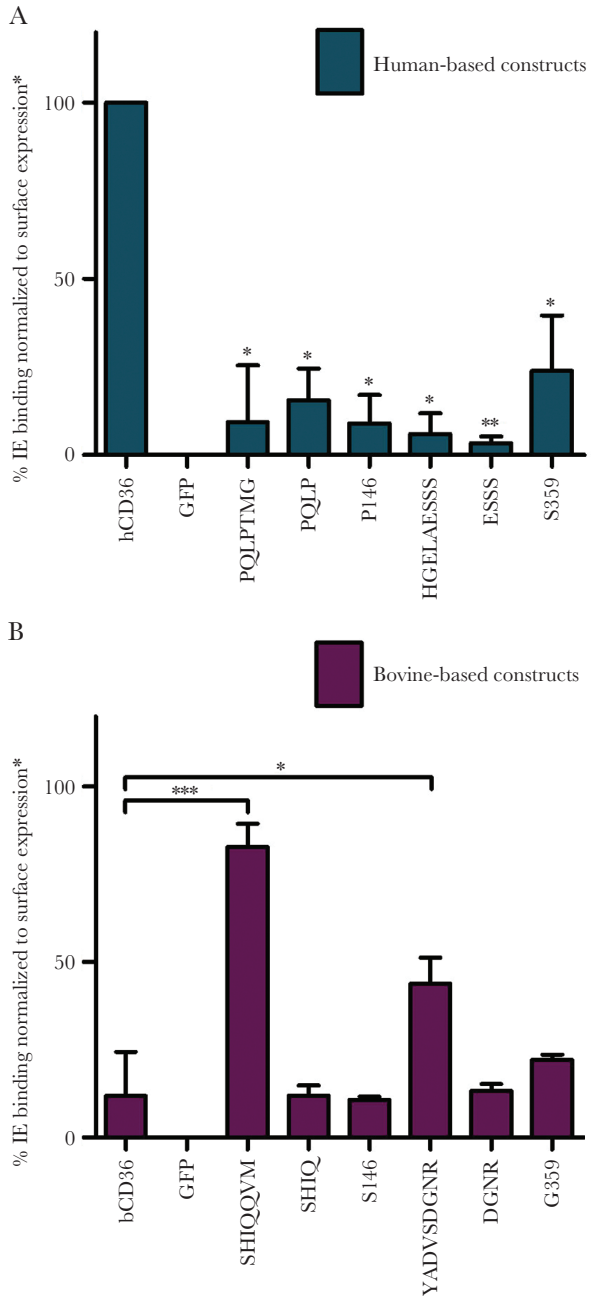

Figure 4. Infected erythrocyte (IE) binding to human- and bovine-based CD36 mutants. (A) Human-based constructs (blue). Quantification of IE binding (mean + standard deviation [SD]) of experiments done in triplicate with statistical significance based on comparison to *h*CD36 wild type (*, $P < .05$). (B) Bovine-based constructs (purple). Quantification of IE binding (mean + SD) of experiments done in triplicate, and statistical significance compared with *b*CD36 wild type (*, $P < .05$ and ***, $P < .0001$). *h*CD36 mutants surface expression were normalized to FA6-152 monoclonal antibody binding, and *b*CD36 mutants surface expression were normalized to CIDRα6_D3_IT4var12 binding (Supplementary Figure 2). GFP, green fluorescent protein.

Role of Serine 146 and Glycine 359 in Infected Erythrocyte Binding

The alignment and binding data suggest that the serine in domain I at position 146 (S146) and the glycine (G359) in domain II may be important for the binding phenotype of *h*CD36. In support of this hypothesis, IE binding by *h*CD36 was abolished when this serine was replaced with the proline found in *b*CD36 (Figure 4A). However, the reciprocal exchange of serine with proline at this position in *b*CD36 did not confer IE binding (Figure 4B). Likewise, point mutation of the glycine at position 359 of the *h*CD36 domain II to the serine found in *b*CD36 significantly decreased binding (Figure 4A), but the converse exchange in *b*CD36 (S359G) did not increase IE binding (Figure 4B). Collectively, these ortholog mutational studies identified residues within domains I and II that are necessary to maintain IE binding in *h*CD36 but were not sufficient to confer binding to *b*CD36. These data suggest that in addition to critical residues, conformational constraints of domains I and II also modify IE interactions.

Analysis of Cysteine-Rich Interdomain Region-α Peptide-CD36 Interactions

As a complementary approach to explore CD36-IE interactions, we used flow cytometry to assess binding by WT and mutant CD36, of CIDRα2 peptides that interact specifically with CD36 or, as a control, the EPCR [24]. In our binding assays, EPCR binding CIDRα1 peptides displayed no affinity for WT or mutant CD36 and served as a negative control for the transfection and binding assays (Figure 5). It is notable that mutations to modify the cationic region in *h*CD36 that abrogated IE binding did not affect CD36 binding of CIDRα2 peptides (Figure 5A). However, *h*CD36 mutants containing domains I and II from *b*CD36, as well as G359S, displayed significantly reduced binding of CIDRα2 peptides similar to that observed with IEs (Figure 5B). CIDRα2 peptides displayed reduced binding to *b*CD36 (Figure 5C and D). Binding was significantly increased when the *b*CD36 domain I was replaced with the corresponding human domain (Figure 5C and D).

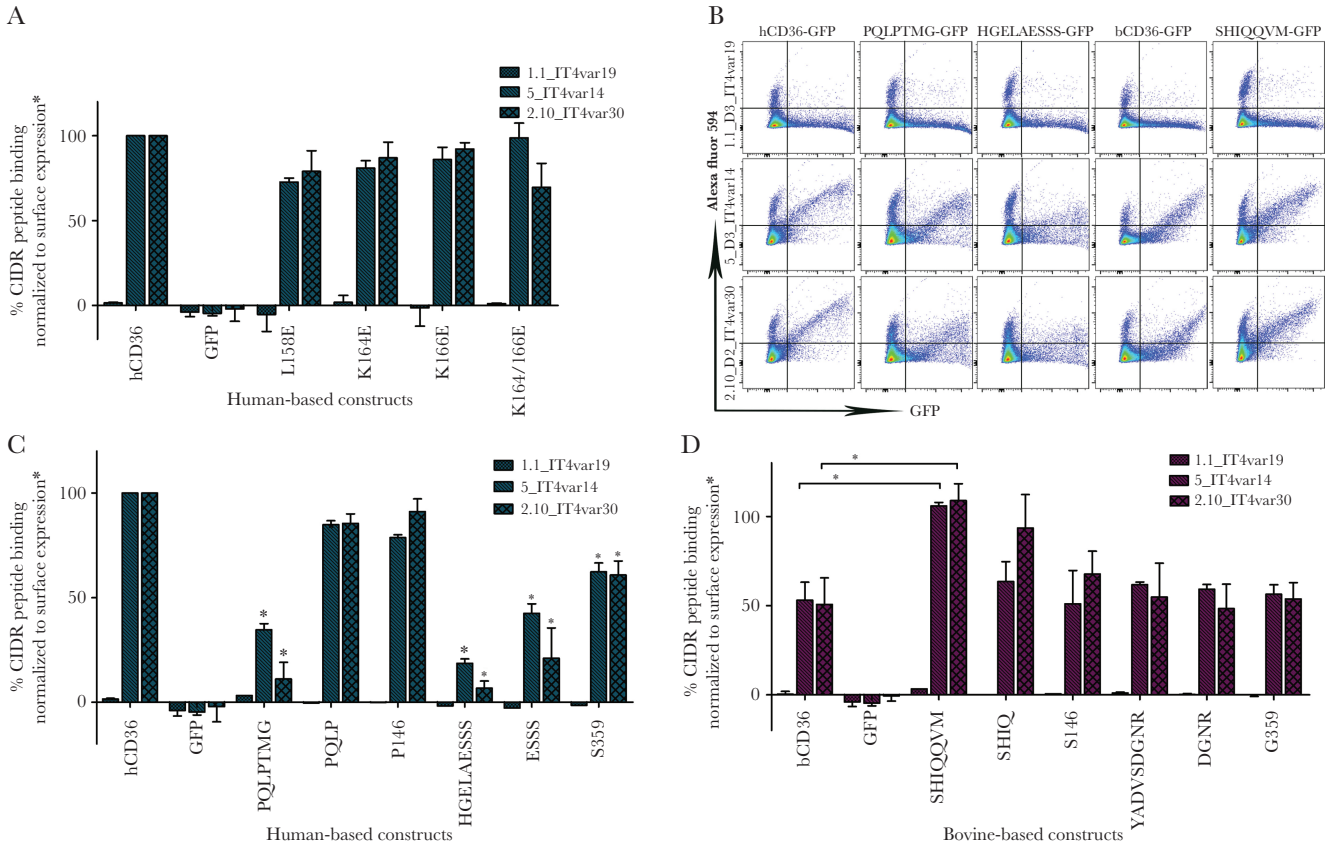

Figure 5. CIDR peptides binding to CD36 mutants. (A) Quantification of peptide binding to *h*CD36 and point mutants by flow cytometry performed in duplicate (mean + standard deviation). Statistical significance compared with *h*CD36 wild type (*, $P < .05$). (B) Flow cytometry charts for selected constructs. (C) Quantification of peptide binding to *h*CD36-based constructs (blue). Statistical significance compared with *h*CD36 wild type (*, $P < .05$). (D) Quantification of peptide binding to *b*CD36-based constructs (purple). Statistical significance compared with *b*CD36 wild type (*, $P < .05$). Surface expression of A was normalized to BD555455 monoclonal antibody binding, *h*CD36 mutants in C were normalized to FA6-152 monoclonal antibody binding, and *b*CD36 mutants in D were normalized to CIDRα6_D3_IT4var12 binding (Supplementary Figure 2). GFP, green fluorescent protein.

Binding of Oxidized Low-Density Lipoprotein, Like Infected Erythrocytes, Is Influenced by hCD36 Domain I and II

As an alternative ligand to IEs, we examined oxLDL binding by the CD36 constructs generated (Figure 6). Exchanging domain I or II in *h*CD36 with the comparable bovine domains, as well as introducing bovine point mutations into *h*CD36 domain I or II, all resulted in significantly reduced oxLDL binding by *h*CD36 (Figure 6). In contrast, replacing *b*CD36 domain I with the *h*CD36 domain increased oxLDL binding to *b*CD36 by 2-fold. Exchange of domain II or other residues within domain II conferred levels of oxLDL binding similar to, or greater than, that of *h*CD36 WT (Figure 6).

DISCUSSION

Solving the crystal structure of LIMP-2 has enabled an improved understanding of the structure of this family of PRRs and how they functionally interact with diverse ligands. Furthermore, the recent cocrystallization of the CD36 ectodomain with PfEMP1 CIDRα2–6 peptides identified a phenylalanine residue at position 153 in *h*CD36 as critical for binding both the oxLDL and CIDRα2–6 domains [9]. In this study, we used the predicted structure of CD36 combined with differential ligand binding by CD36 orthologs to further characterize binding interactions between the biologically relevant ligand (ie, intact IEs) and CD36. Our results provide evidence that the IE interaction with CD36 is dependent on a cationic residue cluster that is influenced by at least 2 additional domains, 1 in proximity and 1 at a distance from this interaction surface.

Although structurally heterogeneous, the CD36 superfamily displays a conserved positively charged region or "cationic patch" that has been implicated in receptor interaction with polyanionic ligands such as modified lipoproteins [10, 13]. In support of this observation, mutating charges within the membrane distal helical bundle region of *h*CD36 (eg, K164E or K166E) have been shown to disrupt oxLDL binding [10, 16]. In this study, we show that these conserved residues are also important for CD36 binding of intact IEs. Although a single charge change in this region is insufficient to disrupt CD36-ligand interactions, a double mutant (K164E and K166E) abrogates binding of both oxLDL and IEs. Collectively, these data

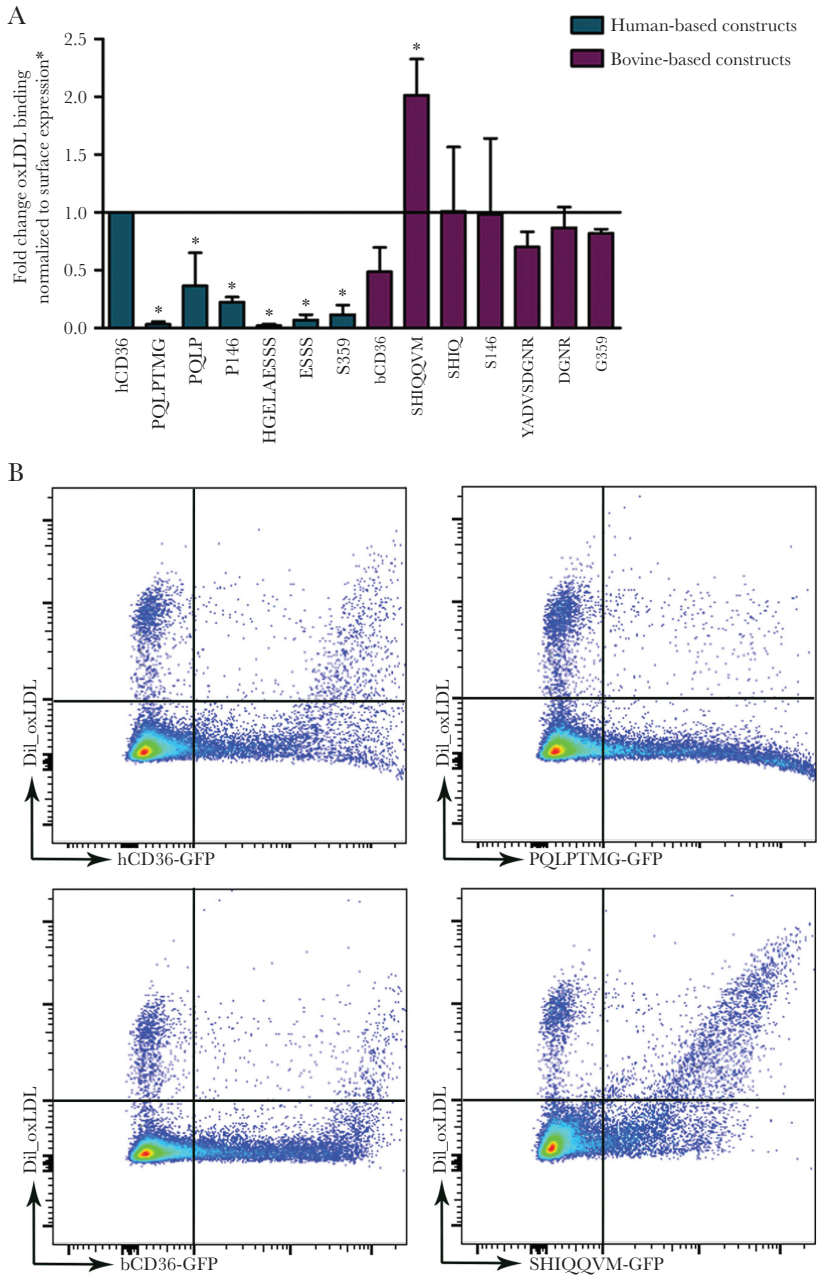

Figure 6. DiI_OxLDL binding. (A) Quantification of oxidized low-density lipoprotein (oxLDL) binding to human-based (blue) and bovine-based (purple) constructs by flow cytometry performed in duplicate (mean + standard deviation) (*, $P < .05$). (B) Flow cytometry charts for selected constructs. *h*CD36 mutant results were surface normalized to FA6-152 monoclonal antibody binding, and *b*CD36 mutants were normalized to CIDRα6_D3_IT4var12 binding (Supplementary Figure 2). GFP, green fluorescent protein.

provide additional evidence supporting the hypothesis that despite structural diversity, a conserved region of shape and electrostatic potential contributes to the broad repertoire of ligands bound by the CD36 superfamily of receptors [10].

Residues within this putative interaction site are necessary for binding; however, their functionality appears to be conformationally constrained. Given the broad and unrelated nature of many of the ligands bound by scavenger receptors, it has been proposed that, in addition to ligand interaction surfaces, other small sequence and structural features will determine the function and regulate differential ligand recognition by this class of receptors. We provide several lines of evidence supporting this hypothesis. First, *b*CD36 has a conserved phenylalanine at 153 (ie, the reported binding site in *h*CD36 for CIDRα2–6 peptides), as well as the same conserved lysine residues at positions 164 and 166 as *h*CD36, but only binds oxLDL approximately 50% as well and binds IEs poorly compared with *h*CD36. Residues predicted to be buried in the helical bundle, L158 and L161, were previously shown to be required for binding of oxLDL and have been proposed to be important for

protein-protein interactions or dimer formation [16]. Of note, L158 is required for IE binding by *h*CD36. Mutations in this area induce allosteric conformational changes on the cationic surface that directly or indirectly disrupt ligand binding.

Second, when the *h*CD36 domain I is introduced to replace the corresponding region in *b*CD36, IE binding to the *b*CD36 backbone is significantly enhanced and comparable to WT *h*CD36. Notably, introducing *h*CD36 domain I to replace the corresponding domain in bovine also results in enhanced binding of oxLDL by *b*CD36, increasing oxLDL binding by 2-fold over WT *h*CD36. However, inserting bovine mutations into domain I and II of *h*CD36 results in decreased oxLDL binding. Collectively, these data suggest that subtle changes in sequence or domain arrangement can alter ligand interaction and selectivity, perhaps by inducing conformation changes that make the interaction surface more or less accessible to the ligand.

Finally, we observed that CD36 binding of CIDRα2 peptides was influenced by domain I and II exchange and specific mutations within these domains. Exchanging bovine domain I with human domain I resulted in 2-fold increase in binding of CIDRα peptides by *b*CD36 and conversely a significant decrease in binding by *h*CD36. Similar to IE binding, introducing bovine domain II, or its associated point mutations, decreased CIDRα2 binding by *h*CD36. However, none of the mutations introduced to alter charge in the cationic region had an impact on binding of CIDRα peptides. Of note, CD36 can recognize and bind hundreds of CIDRα sequences although there is minimal sequence conservation [8]. Our data support the hypothesis that CD36, as a PRR, recognizes the conserved structure of these peptides as PAMPs, and binding is influenced by subtle changes in tertiary structure, rather than by a sequential binding process requiring specific charged residues as was observed for intact IEs.

Collectively, our data suggest a putative model where (1) a charged binding surface on CD36 binds IEs via parasite-encoded domains, and/or modified host molecules and (2) direct binding to F153 by PfEMP1 CIDRα2–6 domains. These interactions collectively increase the avidity to form a stable interaction. Precisely how conformational changes induced by domains I and II influence the selectivity and interaction of CD36 for other ligands remains to be determined.

A limitation of mutational approaches is the potential to introduce structural changes in the receptor that abrogates binding independent of informative changes in binding domains. However, to mitigate these issues, we used small domain exchanges between highly conserved and well expressed orthologs. We confirmed expression and function of CD36 mutants by normalizing for cell surface expression and by gain and loss of function experiments using IE, CIDR peptides, and oxLDL binding and antibody reactivity between the mutant CD36 receptors that underwent reciprocal domain swap exchange.

Immune pressure on CIDRα molecules seems to be responsible for their sequence diversity, but conservation of domain structure is required to bind to the same or similar sites as physiological ligands [25]. This characteristic is shared by other PPRs that recognize diverse ligands through shared structure rather than amino acid sequence. Scavenger receptors are also known for their propensity to oligomerize, favoring binding of large and multivalent ligands [10]. This could certainly be the case for multiple CIDRα domains in PfEMP1 molecules widely distributed on the red blood cell membrane.

CONCLUSIONS

Because CIDRα peptide binding is not dependent upon charge, it is currently unknown what ligand on IEs directly interacts with the charged binding surface. These candidates include other parasite-encoded erythrocyte surface proteins (eg, Clag9) [26, 27], products of oxidation, modification, and degradation of membrane proteins (eg, Band-3, hemichrome formation, CD47) [28–33], or disruption of the phospholipid asymmetry by exposure of phosphatidylserine [34–36]. Further studies are also required to examine the involvement of other IE ligands in CD36 binding, as well as the implications of sequence variations in CD36 on modifying uptake of oxLDL by monocytic cells and whether this plays a role in the pathobiology of atherosclerosis.

Supplementary Data

Supplementary materials are available at *The Journal of Infectious Diseases* online. Consisting of data provided by the authors to benefit the reader, the posted materials are not copyedited and are the sole responsibility of the authors, so questions or comments should be addressed to the corresponding author.

Notes

Disclaimer. The funders had no role in study design, data collection and analysis, decision to publish, or preparation of the manuscript.

Financial support. This work was funded by Canadian Institutes of Health Research (CIHR) Foundation Grant FDN-148439 (to K. C. K.), Canada Research Chair (to K. C. K.), CIHR Postdoctoral Fellowship (to A. C.), The Natural Science Foundation of Zhejiang Province Grant 31770938 (to D. N.), and National Natural Science Foundation of China Grant LZ16C050001 (to D. N.).

Potential conflicts of interest. All authors: No reported conflicts of interest. All authors have submitted the ICMJE Form for Disclosure of Potential Conflicts of Interest.

References

1. Snow RW, Guerra CA, Noor AM, Myint HY, Hay SI. The global distribution of clinical episodes of *Plasmodium falciparum* malaria. Nature **2005**; 434:214–7.
2. Murray CJ, Rosenfeld LC, Lim SS, et al. Global malaria mortality between 1980 and 2010: a systematic analysis. Lancet **2012**; 379:413–31.

3. World Health Organization. World Malaria Report 2016. Geneva: World Health Organization; **2016**.
4. Guizetti J, Scherf A. Silence, activate, poise and switch! Mechanisms of antigenic variation in *Plasmodium falciparum*. Cell Microbiol **2013**; 15:718–26.
5. Scherf A, Lopez-Rubio JJ, Riviere L. Antigenic variation in *Plasmodium falciparum*. Annu Rev Microbiol **2008**; 62:445–70.
6. Kraemer SM, Smith JD. A family affair: var genes, PfEMP1 binding, and malaria disease. Curr Opin Microbiol **2006**; 9:374–80.
7. Mo M, Lee HC, Kotaka M, et al. The C-terminal segment of the cysteine-rich interdomain of *Plasmodium falciparum* erythrocyte membrane protein 1 determines CD36 binding and elicits antibodies that inhibit adhesion of parasite-infected erythrocytes. Infect Immun **2008**; 76:1837–47.
8. Klein MM, Gittis AG, Su HP, et al. The cysteine-rich interdomain region from the highly variable *Plasmodium falciparum* erythrocyte membrane protein-1 exhibits a conserved structure. PLoS Pathog **2008**; 4:e1000147.
9. Hsieh FL, Turner L, Bolla JR, Robinson CV, Lavstsen T, Higgins MK. The structural basis for CD36 binding by the malaria parasite. Nat Commun **2016**; 7:12837.
10. Canton J, Neculai D, Grinstein S. Scavenger receptors in homeostasis and immunity. Nat Rev Immunol **2013**; 13:621–34.
11. Silverstein RL, Febbraio M. CD36, a scavenger receptor involved in immunity, metabolism, angiogenesis, and behavior. Sci Signal **2009**; 2:re3.
12. McGilvray ID, Serghides L, Kapus A, Rotstein OD, Kain KC. Nonopsonic monocyte/macrophage phagocytosis of *Plasmodium falciparum*-parasitized erythrocytes: a role for CD36 in malarial clearance. Blood **2000**; 96:3231–40.
13. Heit B, Kim H, Cosío G, et al. Multimolecular signaling complexes enable Syk-mediated signaling of CD36 internalization. Dev Cell **2013**; 24:372–83.
14. Kobylka D, Carraway KL. Proteolytic digestion of proteins of the milk fat globule membrane. Biochim Biophys Acta **1973**; 307:133–40.
15. Cabrera A, Neculai D, Kain KC. CD36 and malaria: friends or foes? A decade of data provides some answers. Trends Parasitol **2014**; 30:436–44.
16. Neculai D, Schwake M, Ravichandran M, et al. Structure of LIMP-2 provides functional insights with implications for SR-BI and CD36. Nature **2013**; 504:172–6.
17. Trager W. *Plasmodium falciparum* in culture: improved continuous flow method. J Protozool **1979**; 26:125–9.
18. Dorrington MG, Roche AM, Chauvin SE, et al. MARCO is required for TLR2- and Nod2-mediated responses to *Streptococcus pneumoniae* and clearance of pneumococcal colonization in the murine nasopharynx. J Immunol **2013**; 190:250–8.
19. Chaiyaroj SC, Coppel RL, Novakovic S, Brown GV. Multiple ligands for cytoadherence can be present simultaneously on the surface of *Plasmodium falciparum*-infected erythrocytes. Proc Natl Acad Sci U S A **1994**; 91:10805–8.
20. Serghides L, Crandall I, Hull E, Kain KC. The *Plasmodium falciparum*-CD36 interaction is modified by a single amino acid substitution in CD36. Blood **1998**; 92:1814–9.
21. Baruch DI, Ma XC, Pasloske B, Howard RJ, Miller LH. CD36 peptides that block cytoadherence define the CD36 binding region for *Plasmodium falciparum*-infected erythrocytes. Blood **1999**; 94:2121–7.
22. Ockenhouse CF, Tandon NN, Jamieson GA, Greenwalt DE. Antigenic and functional differences in adhesion of *Plasmodium falciparum*-infected erythrocytes to human and bovine CD36. Infect Immun **1993**; 61:2229–32.
23. Garnier J, Gibrat JF, Robson B. GOR method for predicting protein secondary structure from amino acid sequence. Methods Enzymol **1996**; 266:540–53.
24. Turner L, Lavstsen T, Berger SS, et al. Severe malaria is associated with parasite binding to endothelial protein C receptor. Nature **2013**; 498:502–5.
25. Lau CK, Turner L, Jespersen JS, et al. Structural conservation despite huge sequence diversity allows EPCR binding by the PfEMP1 family implicated in severe childhood malaria. Cell Host Microbe **2015**; 17:118–29.
26. Ockenhouse CF, Klotz FW, Tandon NN, Jamieson GA. Sequestrin, a CD36 recognition protein on *Plasmodium falciparum* malaria-infected erythrocytes identified by anti-idiotype antibodies. Proc Natl Acad Sci U S A **1991**; 88:3175–9.
27. Holt DC, Gardiner DL, Thomas EA, et al. The cytoadherence linked asexual gene family of *Plasmodium falciparum*: are there roles other than cytoadherence? Int J Parasitol **1999**; 29:939–44.
28. Winograd E, Sherman IW. Malaria infection induces a conformational change in erythrocyte band 3 protein. Mol Biochem Parasitol **2004**; 138:83–7.
29. Crandall I, Sherman IW. *Plasmodium falciparum* (human malaria)-induced modifications in human erythrocyte band 3 protein. Parasitology **1991**; 102 Pt 3:335–40.
30. Wolofsky KT, Ayi K, Branch DR, et al. ABO blood groups influence macrophage-mediated phagocytosis of *Plasmodium falciparum*-infected erythrocytes. PLoS Pathog **2012**; 8:e1002942.
31. Crandall I, Collins WE, Gysin J, Sherman IW. Synthetic peptides based on motifs present in human band 3 protein inhibit cytoadherence/sequestration of the malaria parasite *Plasmodium falciparum*. Proc Natl Acad Sci U S A **1993**; 90:4703–7.
32. Banerjee R, Khandelwal S, Kozakai Y, Sahu B, Kumar S. CD47 regulates the phagocytic clearance and replication of the *Plasmodium yoelii* malaria parasite. Proc Natl Acad Sci U S A **2015**; 112:3062–7.

33. Ayi K, Lu Z, Serghides L, et al. CD47-SIRPα interactions regulate macrophage uptake of *Plasmodium falciparum*-infected erythrocytes and clearance of malaria In Vivo. Infect Immun **2016**; 84:2002–11.
34. Setty BN, Kulkarni S, Stuart MJ. Role of erythrocyte phosphatidylserine in sickle red cell-endothelial adhesion. Blood **2002**; 99:1564–71.
35. Walker B, Towhid ST, Schmid E, et al. Dynamic adhesion of eryptotic erythrocytes to immobilized platelets via platelet phosphatidylserine receptors. Am J Physiol Cell Physiol **2014**; 306:C291–7.
36. Greenberg ME, Sun M, Zhang R, Febbraio M, Silverstein R, Hazen SL. Oxidized phosphatidylserine-CD36 interactions play an essential role in macrophage-dependent phagocytosis of apoptotic cells. J Exp Med **2006**; 203:2613–25.